Published in "Deep Sea Research Part II: Topical Studies in Oceanography 171(): 104664, 2020" which should be cited to refer to this work.

Preliminary video-spatial analysis of cold seep bivalve beds at the base of the continental slope of Israel (Palmahim Disturbance)

V. Beccari [a,*], D. Basso [b], S. Spezzaferri [a], A. Rüggeberg [a], A. Neuman [c], Y. Makovsky [c]

[a] University of Fribourg, Department of Geosciences, Chemin du Musée 6, 1700, Fribourg, Switzerland
[b] University of Milano - Bicocca, Department of Earth and Environmental Sciences, (CoNISMa, ULR), Piazza della Scienza 4, 20126, Milano, Italy
[c] Dr. Moses Strauss Department of Marine Geosciences and Hatter Department of Marine Technology, Leon H. Charney School of Marine Sciences (CSMS), University of Haifa, Haifa, 31905, Israel

ARTICLE INFO

Keywords:
Cold seep
Chemosynthesis
Gas emissions
Bivalve
Lucinoma kazani
Eastern Mediterranean basin

ABSTRACT

Seafloor video surveys were carried out with the ROV Max Rover in the Palmahim Disturbance (PD) area, offshore Israel, in September 2016 during the EUROFLEETS2 SEMSEEP cruise on board the R/V AEGAEO. Preliminary observations of distribution and frequencies of bivalve accumulations show that they are mostly composed by *Lucinoma kazani* shells. Valves are distributed mainly along the base of authigenic carbonate crusts, in association with bacterial mats and inside inactive chimney-like structures, sometimes associated with crabs and living tubeworms. However, no living molluscs were observed.

The relation between distribution of bivalve beds and seepage activity is not straightforward in the PD area. However, the presence of these accumulations and the size of *L. kazani*, suggest that seepages may have lasted for at least one decade, before its reduction/cessation that induced *L. kazani* mortality. The presence of few articulated valves of this species indicates that they were alive up to one year before the ROV observations and their different preservation state may imply different seepage phases. This research shows that chemosymbiotic benthic communities may be used as a proxy for better understanding the past dynamics of fluid emissions at the seafloor. However, further quantitative studies are needed to confirm these observations.

1. Introduction

Cold seep environments have been identified in the world's oceans, along passive and active margins from shallow to bathyal depths (e.g., Paull et al., 1984; Sibuet and Olu-Le Roy, 2002; Levin, 2005), and are associated with morphological features such as pockmarks, mud volcanoes and brine pools (Taviani et al., 2013, 2014, and reference therein). At seeps and vents, fluids enriched by dissolved reducing gas support the microbial chemosynthetic processes (e.g., Sahling et al., 2002; Boetius and Wenzhöfer, 2013) and specialized metazoan communities, dominated by few adapted taxa (e.g., Ritt et al., 2010). Cold seeps communities are characterized by high biomass of clams, mussels, siboglinid tubeworms and sulphur-oxydizing bacterial mats (e.g., Van Dover et al., 2003; Cordes et al., 2010; Levin et al., 2016) clustered in high density or spread in large fields (Vanreusel et al., 2009).

The anaerobic oxidation of methane (AOM) and other hydrocarbons causes the release of hydrogen sulfide and bicarbonate into the pore water, increasing the alkalinity (Boetius et al., 2000; Ritger et al., 1987; Blumenberg, 2015) and inducing the formation of authigenic carbonate crusts and concretions in anoxic sediments (Barnes and Goldberg, 1976; Foucher et al., 2009). Chemoautotrophic species e.g., sulphur bacteria, and/or chemoautotrophic symbiont-bearing invertebrates, such as bivalves, use the sulfide produced in these environments (Sahling et al., 2002, and reference therein). Where photosynthesis cannot occur, the available food is sustained by planktonic production at surface waters, organic carbon produced in shallow coastal environment and transferred to depth by sediment transport (detritus-based communities: Suess, 1980; Boetius et al., 2000; Sibuet and Olu-Le Roy, 2002) and/or by chemosynthesis (chemosymbiotic communities: Corselli and Basso, 1996; Sibuet and Olu-Le Roy, 2002; Taviani, 2014; Kiel, 2016 and reference therein).

The presence and the abundance of large siboglinid tubeworms (Siboglinidae polychaetes), chemosymbiotic bivalves and bacterial mats are some of the best indicators and tracers of current methane-rich fluid emissions at the seafloor, whereas massive carbonate crusts and clusters of siboglinid tubeworms may indicate long-term, presently episodic

* Corresponding author.
E-mail address: valentina.beccari@unifr.ch (V. Beccari).

seepage (Sibuet and Olu-Le Roy, 2002; Zitter et al., 2005). Following Sibuet and Olu-Le Roy (2002), the variability of chemosymbiotic macrofauna among sites may be explained by several factors, such as depth and habitat heterogeneity. The concept of habitat heterogeneity includes geology, geometry of seeps, pattern and volume of fluid flow and occurrence of gas hydrates. Local geology can influence methane and oxygen concentrations, intensity and pathways of fluid emission in the seeps, controlling, together with microbial activity, the lateral and vertical extent of the authigenic carbonate constructions on the seafloor (e.g., Aloisi et al., 2002; Olu-Le Roy, 2007; Gontharet et al., 2007; Taviani, 2014, and reference therein).

According to the concept of habitat heterogeneity, faunal composition, abundance and distribution are also influenced by fluid emission intensity and continuity, sulfide concentration, and their gradients within the sediment (Huguen et al., 2009; Zitter et al., 2005; Ritt et al., 2011; Zeppilli et al., 2012). This biological zonation has been observed in several locations, e.g., the Amsterdam Mud Volcano (Olu-Le Roy et al., 2004) and the Barbados prism (Olu et al., 1997), where the top of the mud volcanoes is covered by sulphide-oxydizing bacterial mats with an increasing number of symbiont-bearing and heterotrophic fauna toward the peripheries (e.g., Olu et al., 1997; Zitter et al., 2005; Ritt et al., 2011, and reference therein).

Deep-sea communities were initially discovered only in association with hydrothermal sulphuric emissions, e.g., *black smokers,* in the offshore of Galapagos (Lonsdale, 1977). Successive researches revealed chemosymbiotic communities on the Florida escarpment, associated with cold seeps environments (Paull et al., 1984). These communities have been described on mud volcanoes, cold seeps and hydrothermal vents in the Mediterranean Sea (e.g., Corselli and Basso, 1996; Woodside et al., 1998; Taviani, 2014).

The Eastern Mediterranean is an important hotspot of methane seepage features (Ritt et al., 2011, and reference therein) in particular, on the Mediterranean Ridge and in the Nile Deep Sea Fan (e.g., Loncke et al., 2006; Ritt et al., 2011). The formation of hydrocarbons in deep reservoirs is probably due to the accumulation of organic-rich sediments since the early Cenozoic, after sealing by the thick Messinian evaporites (Hsü et al., 1977). Several locations are known nowadays in the easternmost part of the Mediterranean Basin to host chemosymbiotic communities (e.g., Corselli and Basso, 1996; Olu-Le Roy et al., 2004; Taviani, 2014; Rubin-Blum et al., 2014; Makovsky et al., 2017).

In the Nile Deep Sea Fan, deep Mediterranean chemosymbiotic bivalves of the families Vesicomyidae, Lucinidae, Thyasiridae and Mytilidae were recovered for the first time in the nineteenth century by the Austro-Hungarian ship *Pola* (Sturani, 1896). Corselli and Basso (1996) for the first time documented lucinids-vesicomyids fauna from the Napoli mud volcano on the Mediterranean Ridge. Benthic macrofauna is patchily distributed in this region, that is otherwise defined as a marine benthic desert due to deep oligotrophic waters and paucity of organic matter potentially conveyed from shelf areas (Basso et al., 2004). The typical environment of Lucinidae is gas-saturated mud, with high sulphide and low oxygen levels in deep-sea environments (Salas and Woodside, 2002). The chemosymbiotic bivalve *Lucinoma kazani* is nowadays considered as the main component of living cold seep communities in the Eastern Mediterranean Sea (Salas and Woodside, 2002; Olu-Le Roy et al., 2004; Werne et al., 2004) and according to Ritt et al. (2011) it provides indirect evidences of seepage, as it is often associated with rich organic matter and sulphidic sediments.

2. Seepage in the Southeastern Levantine Basin

The Levantine Basin, located at the southeastern corner of the Mediterranean Sea, is controlled by Nilotic supplies of sediments and nutrients, it is ultra-oligotrophic and is extremely sensitive to climatic changes (e.g., Almogi-Labin et al., 2009). The basin floor is directly supplied by a dense net of turbidite channels of the Nile Deep Sea Fan, the most western of them being the apparently currently inactive Levant

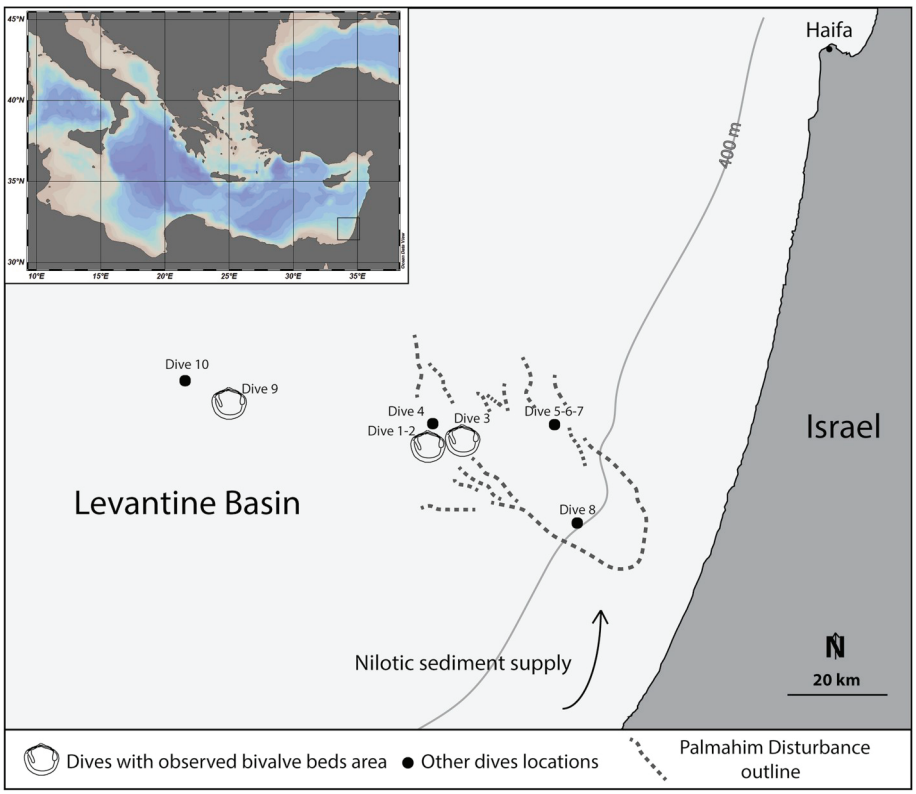

Fig. 1. Location map of the Israeli coast and PD area showing the locations of the 2016 SEMSEEP cruise ROV dives. The inset shows the study area in the context of the Eastern Mediterranean Sea (modified from Ocean data view website, Schlitzer, R., Ocean Data View, https://odv.awi.de, 2018).

Channel (Gvirtzman et al., 2015). The southeastern Levant seafloor is prominently deformed due to continued thin skin mobilization of the Messinian evaporites ~1 km beneath the seafloor, forming sets of faults and ridges (e.g., Gvirtzman et al., 2015, and references therein). The Palmahim Disturbance (PD) is a large-scale (15 x 50 km) rotational slide impacting the continental shelf and slope of southern Israel (Garfunkel et al., 1979).

A variety of seepage related features, including active cold seeps, were discovered and investigated along the base of the Israeli continental slope in the course of E/V Nautilus 2010, 2011 ROV surveys (Coleman et al., 2012) and the SEMSEEP EUROFLEETS2 cruise onboard the R/V Aegaeo (Makovsky et al., 2017). Most of the active seepage sites are concentrated at water depths of 1100–1300 m in the western toe region of PD (e.g., Fig. 1). Additional seepage sites were investigated within the Levant Channel at the western bound of PD (Fig. 1, Dive 1), and in a major pockmarks system etched within a thin skin fold ridge in Gal-C exploration block, ~40 km to the west (Fig. 1, Dive 9). These seepage sites are associated to hundreds-of-meters-scale seafloor pockmarks, carbonate buildups, intense seafloor perturbations and a variety of chemosymbiotic fauna. Short sediments cores, one of them collected at a water depths of ~1100 m in one of the PD seepage sites, portray high concentrations of microbial methane (Rubin Blum et al., 2014).

Here we present preliminary observations of the distribution and frequencies of bivalve associated with benthic communities at the sites investigated in during the SEMSEEP cruise and propose that they can be used to trace spatial seepage occurrence and activity in the region.

3. Material and methods

3.1. Analysed material

In this research, we trace the distribution of chemosymbiotic bivalves based on ROV videos, taken in September 2016 during the EUROFLEETS2 SEMSEEP cruise on board the R/V AEGAEO near the base of the Mediterranean continental slope of Israel (Makovsky et al., 2017). The ROV Max Rover was tracked with a Link-quest Tracklink 10000 system. The videos used in this work were acquired with two OceanPro HD cameras (1920x1080), one a general purpose wide-angle camera and the other a macro-zoom camera, mounted on a pan and tilt in the front of the ROV. Lighting was provided by two forward-down angled HID lights and four halogen lights. Two laser beams 10 cm apart provided the distance scale.

Ten dives were analysed (Table 1), with a total of 47 h of dive time and a total length of 50 km, over 5 sites at a water depth ranging from 439 m to 1241 m. However, only the dives (dives 1–2 are from now considered as one because they refer to the same site) showing accumulation of bivalves (hereafter called bivalve beds) and other evidence of recently active seeps are here analysed.

We target bivalve beds, in relation to the type of substrate and the adjacent environment (Figs. 2 and 3; Table 2). The area of bivalve beds was measured with the software ImageJ and scaled by the laser beams (Supplement_material A). Where the laser beams were not visible, we used shells or the arm of the ROV sampler as a scale. The area where the bivalve beds settled was delimited and estimated and all observed shells were counted. Each valve was counted as one and, accordingly, each articulated bivalve shell was counted as one individual with two valves (Scarponi and Kowalewski, 2004; Basso and Corselli, 2007). The preservation degree of *Lucinoma kazani* shells collected during this expedition was evaluated using the taphonomic grade of preservation of molluscs of Davies et al. (1990) and later elaborated by Basso and Corselli (2007). A qualitative analysis of the faunal assemblages described in these areas is reported by Basso et al. (submitted).

4. Results

A total area of about 208.4 m^2 of dead bivalve beds is identified at water depths from ~1000 to 1250 m. Dive routes, bathymetry, bivalve beds, site locations, color and size-coded for substrate and number of shells are shown in Fig. 3. Most of the observed shells are estimated to be about 3–4 cm in length, and disarticulated. Only in a few cases the valves are articulated and well preserved (Fig. 2; Table 2; Supplementary Material B). Fragments of unidentified large shells are locally abundant (e.g., Dive 3). These are tentatively attributed to *Lucinoma kazani*, since this is the only species known in the area able to produce shells and fragments with the observed sizes. The preservation state of shells includes different taphonomic grades, from fresh to strongly corroded, especially on the ventral margins as shown in Fig. 4. The luster may be preserved (Fig. 4.1a), or completely lost, while the shell color gradually fades towards grey and brownish (Figs. 4.2-3). Bioencrustation by tiny tube-welling organisms is also observed (Fig. 4.3a–b). The plot of the valve numbers against the area of each observed sites (Fig. 5) does not reveal a clear connection between them. Therefore, there seems to be a threshold density of ~200 valves/m^2, which was exceeded only in one site of Dive 9. However, it is not clear if this threshold is an artefact due to measurement methodology. In addition, no clear causal link is observed between substrate and distribution of bivalve beds.

4.1. Seeps within the Levant Channel (dive 1)

During Dive 1 (Fig. 3 a-b) near the toe of the PD bioturbation is rare

Table 1
Representative coordinates, depths and presence or absence of bivalve beds for the 2016 SEMSEEP cruise ROV dives.

ROV dive	Latitude (N)	Longitude (E)	Max depth (m)	Bivalve beds (y/n)
1	Start 32°09.749′	34°06.867′	1234	yes
	End 32°09.839′	34°06.964′		
2	Start 32°09.866′	34°06.897′	1232	yes
	End 32°09.857′	34°06.922′		
3	Start 32°09.458′	34°10.113′	1047	yes
	End 32°09.778′	34°09.905′		
4	Start 32°10.369′	34°07.845′	1249	no
	End 32°10.054’	34°08.010′		
5	Start 32°09.668′	34°23.388′	705	no
	End 32°09.668′	34°23.396′		
6	Start 32°09.579′	34°23.192′	747	no
	End 32°09.192′	34°23.535′		
7	Start 32°09.635′	34°23.329′	746	no
	End 32°09.579′	34°23.425′		
8	Start 32°01.796′	34°23.558′	439	no
	End 32°01.398′	34°23.028′		
9	Start 32°14.341′	33°42.974′	1171	yes
	End 32°14.895’	33°42.404′		
10	Start 32°15.209′	33°37.141′	1180	no
	End 32°15.459’	33°37.459′		

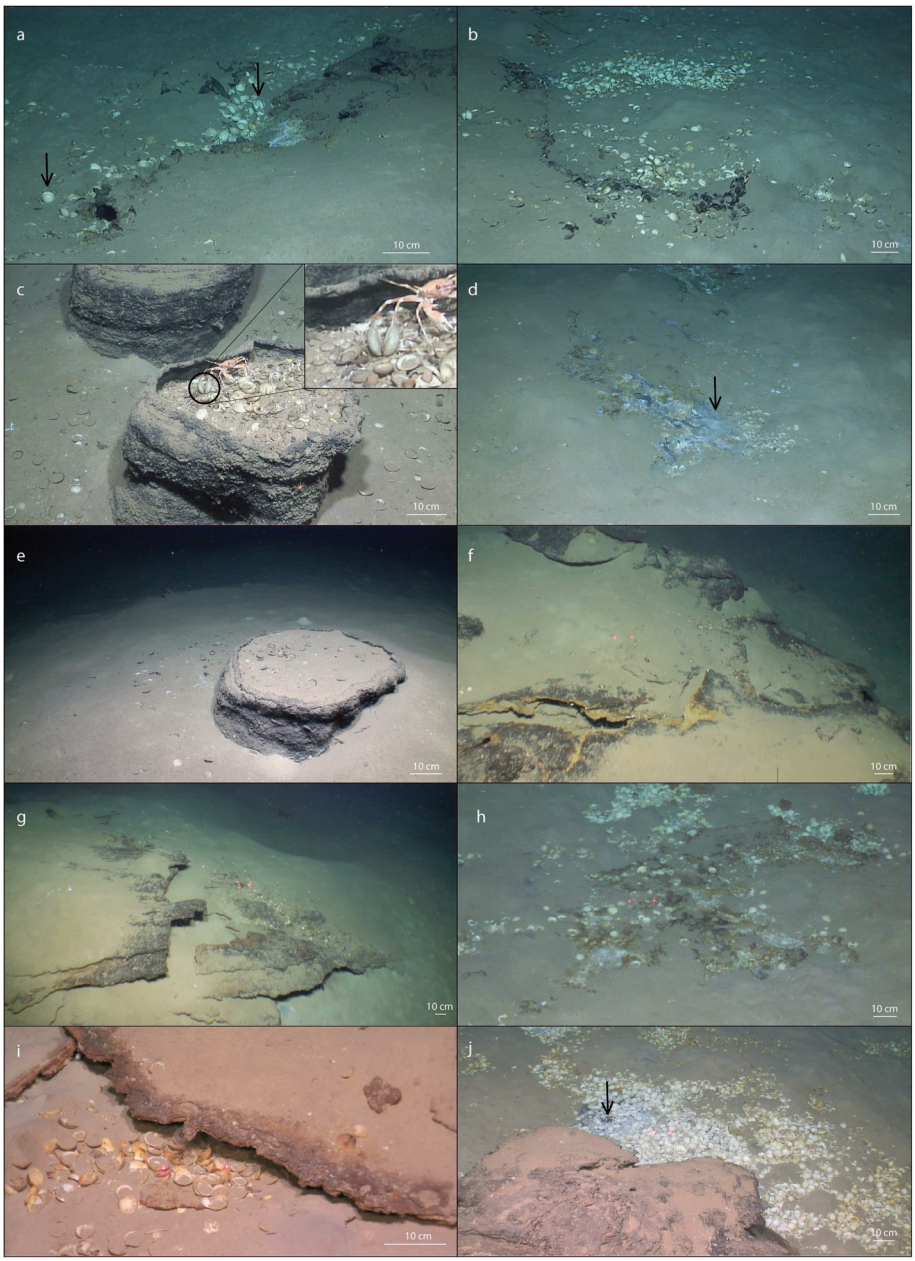

Fig. 2. Examples of the surveyed sites showing bivalve beds and proximate substrates, including carbonate crusts, chimney-like structures, bacterial mats and altered sediments (bluish spots pointed by the arrow in image d and j). a-e (Dive 1); f-g (Dive 3); i-j (Dive 9). Note an articulated dead bivalve (arrows in image a and circle in image c).

to abundant, forming in some cases decimeter-sized mounds. Three inactive chimney-like structures filled with sediments and bivalve shells were observed along the track (Fig. 2c–e). The bivalve shells observed in this area are accumulated around or inside the chimney-like structures (Sites 1 d, 3 Fig. 2c–e), close to the authigenic carbonate crusts (Site 1c), above the grey patches (Sites 1b, 2, 4, 5, Fig. 2d) and sparse on the seafloor (Site 1a).

We identified eight sites within the Levant Channel (Table 2, Supplementary material B). Some of the sites are characterized by bivalve aggregates above grey patches, marking a change in the sediment color from brownish to yellow-blue and possibly indicating methane emission with the subsequent development of microbial mats (Fig. 2d). The estimated total area of the Levant Channel sites is about 28 m^2, the total number of counted shells is 1993 with mean density of 90 valves m^{-2}. The bivalve beds are close to the chimney-like structures or on bacterial mats, which may represent sub-recent hotspots of biodiversity in this extreme environment, now inactive and filled with sediment.

Bivalve assemblages are dominated by *L. kazani*. Most of the valves are disarticulated, but well preserved. Some valves are still articulated due to ligament preservation. Almost all of the articulated bivalves are above or close to the chimney-like structure, where also a crab was observed (Fig. 2c).

4.2. *Palmahim pockmark and Palmahim Disturbance (dive 3)*

The estimated area of the bivalve beds for Dive 3 (Fig. 3c–d) in the PD pockmark site is about 14 m^2, the total number of counted bivalve shells is 693 and the average bivalve density is 83.3 valves m^{-2}. This area hosts various undisturbed and/or highly bioeroded chemoherms, consisting of authigenic carbonate crusts (Sites 7–11, Fig. 2f–g). It hosts large communities of living organisms, including anemones, crabs, bivalves and living tubeworms (Sites 8–10). The dead bivalve beds in this

Table 2
Detailed description of fauna and substrate at sites and sub-sites. *n.d. refers to inadequate video quality preventing the counting of shells.

		Site		Area (m^2)	Counted shells	Total ratio (valves/m^2)	Substrate
Dive	**1**	**1**	**1a**	3	163	54	Sparse shells accumulation on the seafloor.
Station	**Levant Channel**		**1b**	4	130	33	Bacterial mats. Sediment colour blue-yellow-white.
			1c	3	368	123	Authigenic carbonate crusts. Articulated bivalve shells.
Latitude	**32°09.866′N**		**1d**	5	616	123	Chimney like structures, and spread accumulation on the surrounding seafloor. Articulated bivalve shells.
Longitude	**34°06.915′E**	**2**		4	465	116	Bacterial mats.
Depth (m)	**1241**	**3**		1	134	134	Chimney-like carbonate structure.
		4		2.5	117	47	Bacterial mats.
		5		5.5	n.d.	n.d.	Bacterial mats.
				28	**1993**	**90.0**	**Total values of area, counted shells and density**
Dive	**3**	**7**	**7a**	3	106	35	Authigenic carbonate crusts and sparse accumulation on the seafloor.
Station	**Palmahim pockmark**		**7b**	6	119	20	Large authigenic carbonate crusts (12.5 m^2), Living tubeworms, anemones and crabs.
		8		1.5	149	99	Large authigenic carbonate crusts (6.5 m^2). Living tubeworms at the base of the crusts. Spots of darker sediments.
Latitude	**32°09.652′N**	**9**		2	114	57	Large authigenic carbonate crusts (11 m^2). Living tubeworms.
Longitude	**34°10.066′E**	**10**		0.5	n.d.	n.d.	Authigenic carbonate crust.
Depth (m)	**1047**	**11**		1	205	205	Large authigenic carbonate crust (12 m^2). Most shells accumulated at the carbonate crust base.
				14	**693**	**83.3**	**Total values of area, counted shells and density**
Dive	**9**	**12**	**12a**	4	402	101	Authigenic carbonate crusts and shells sparse on the seafloor. Well preserved
Station	**Gal C pockmarks**		**12b**	2	754	377	articulated and poorly preserved bivalves. Fishes, crabs and tubeworms. Bioturbated sediment, no bacterial mats.
			12c	1.5	261	174	
			12d	n.d.	n.d.	n.d.	Authigenic carbonate crusts.
			12e	1	n.d.	n.d.	
			12f	0.4	18	45	
		12	**12.1a**	6.5	n.d.	n.d.	Wide area (49m^2) with authigenic carbonate crusts and sparse shells on the seafloor,
Latitude	**32°14.341′N**		**12.1b**	4.5	373	83	in some cases old, possibly reworked.
			12.1c	1.2	83	69	
Longitude	**33°42.974′E**		**12.1d**	3	259	86	
Depth (m)	**1171**		**12.1e**	4	548	137	
			12.1f	n.d.	n.d.	n.d.	
		13	**13a**	2	n.d.	n.d.	Authigenic carbonate crusts and a crust with visible stratification. Low density shells
			13b	6.5	214	33	accumulation on the seafloor.
		14	**14a**	6.5	69	11	Authigenic carbonate crusts partially buried by sediments and shells sparse on the seafloor.
			14b	0.5	44	88	
		15		2.5	70	28	Authigenic carbonate crusts.
		16		9.5	622	65	Authigenic carbonate crusts, with preserved stratification. Crabs, tubeworms, and echinods. Bacterial mats.
		17	**17a**	4	84	21	Sparse shells (old, reworked) on bioturbated sediments.
			17b	0.3	58	193	bivalve shells on altered sediment
		18		8	521	65	Authigenic carbonate crusts and bacterial mats. Living tubeworms.
		19		21	2048	98	Wide area with authigenic carbonate crusts, bioturbated sediment and bacterial mats. Several articulated bivalves.
		20	**20a**	8	748	94	Authigenic carbonate crusts.
			20b	1	n.d.	n.d.	Sparse shells on the seafloor close to carbonate crusts.
		21		1.5	187	125	Authigenic carbonate crusts.
		22		1	n.d.	n.d.	Small patches of altered sediments co-occuring with bacterial mats.
		23		45.5	5210	115	Wide area with authigenic carbonate crusts and bacterial mats. No defined clusters are observed.
		24		4	175	44	Authigenic carbonate crusts. Articulated bivalves.
		25	**25a**	1	n.d.	n.d.	Wide area with authigenic carbonate crust and altered sediment. Bivalves co-existing
			25b	1.5	n.d.	n.d.	with crabs and echinods. Articulated bivalves.
			25c	2	356	178	
			25d	3	453	151	
			25e	1	210	210	
			25f	1	57	57	
		26	**26a**	5	112	22	Authigenic carbonate crusts and altered sediments. Articulated bivalves.
			26b	2	n.d.	n.d.	
				166	**13936**	**103**	**Total values of area, counted shells and density**

area are small and sparse, around and above carbonate crusts (Fig. 2f–g). Articulated valves are not observed. No shells are visible in bioturbated sediments and grey patches. A few additional authigenic carbonate accumulations with small fragments of bivalve shells were observed, but the quality of the images and the small size of the shells do not allow their identification.

4.3. Gal C pockmarks (dive 9)

Dive 9 (Fig. 3e–f) surveyed a pockmark site in a northwest trending thin skin fold ridge. A bioturbation gradient is observed ranging from low to high grade. Wide areas characterized by carbonate crusts (less eroded than in dive 1–2 with stratification still visible) are associated with bivalve beds along their base (Fig. 2h–j). The surface covered by

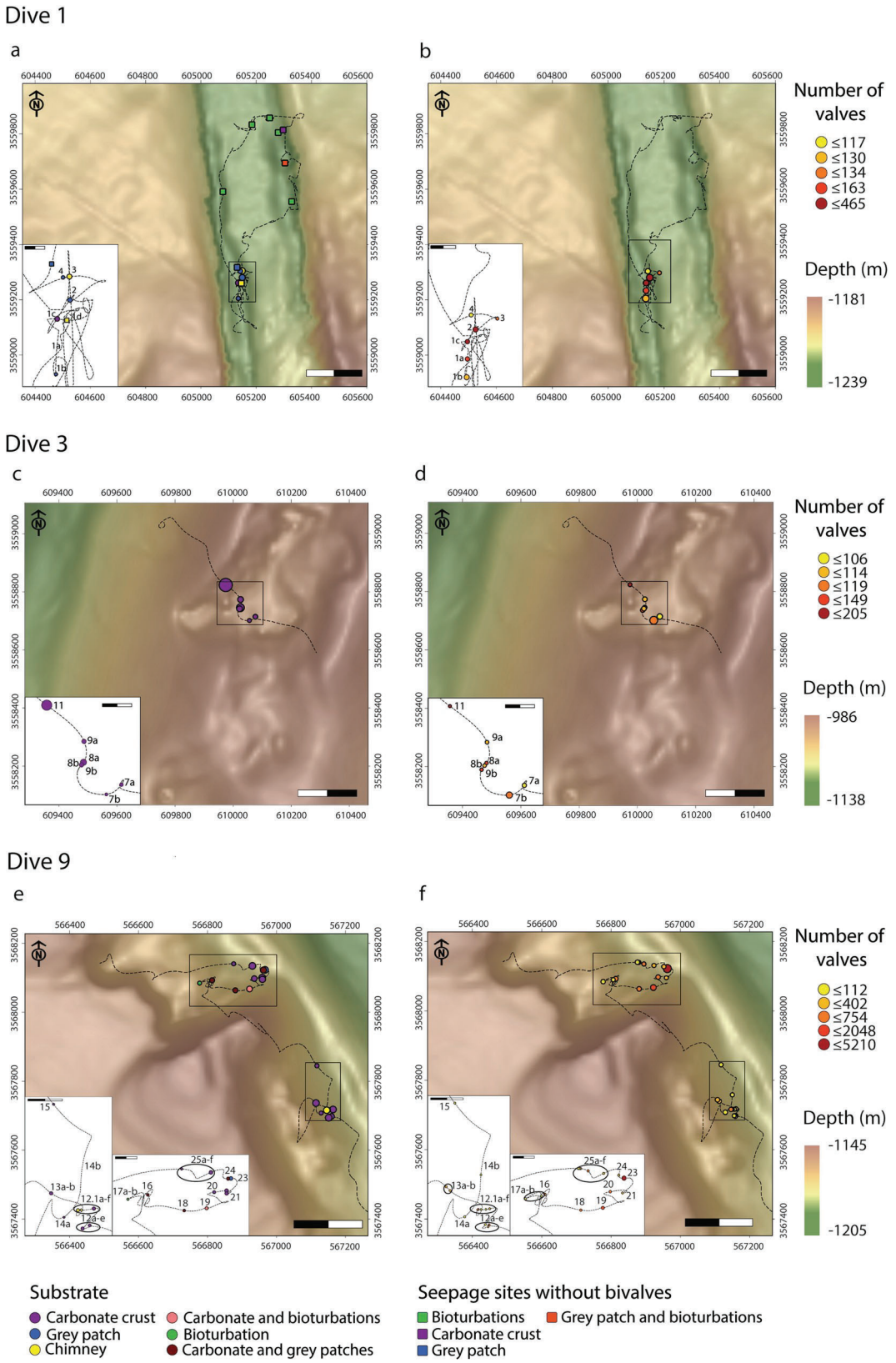

Fig. 3. Habitat maps of the ROV dives. Gradient shaded bathymetric maps of the sites of the 2016 SEMSEEP cruise ROV Dive 1 (Levant Channel; a-b) Dive 3 (PD pockmark; c-d) and Dive 9 (Gal-C pockmarks doublet; e-f), overlaid with the dive route (dashed thin lines). Elevations are optimized in each of the maps (as labeled in the color bars). The observation sites (Table 1) with (circle) and without (squares) valves are color coded by the associated substrate (left; a-c-e) and number of valves (right; b-d-f); and scaled by the ratio of valve number to site area (left; a-c-e) and the site area (right; b-d-f). Zoomed maps of the bivalve site clusters (black frames) are displayed in the bottom left. Distance scale bars plotted are 200 m long for the main maps and 40 m in the zoomed maps. (For interpretation of the references to color in this figure legend, the reader is referred to the Web version of this article.)

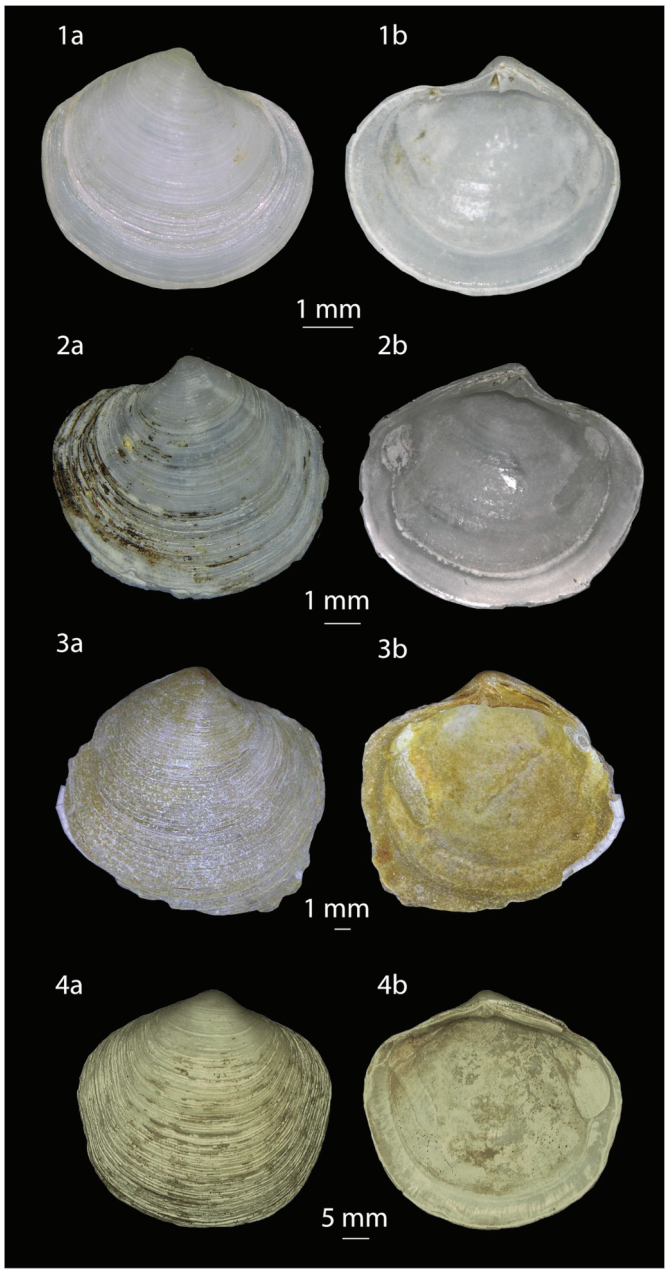

Fig. 4. Size and preservation of *Lucinoma kazani* from pockmark samples SEMSEEP 2016 Cruise. (1–3) Preservation degree is defined according to Basso and Corselli (2007) from (1a-b) taphonomic grade 3, well preserved, disarticulated, to (3a-b) taphonomic grade 1, very bad preservation, broken, brownish shell. (1–4) Different growth stage, from juvenile specimens (1–3) to adult (4).

dead bivalves is the largest observed, being approximately 151 m^2. The total number of counted valves is 13963 with an average density of 103 valves m^{-2}. Several wide distributions of bivalve beds associated with extensive carbonate crusts, were observed covering surface areas reaching around 21 m^2 and 45.5 m^2. In some cases, e.g., for Site 23, an extensive area of carbonate crusts and shells was defined as one site, because it was impossible to define single clusters (Table 2; Supplementary material B).

The bivalve beds are located above and along the edge of carbonate crusts (Fig. 2i–j), where they are partially covered by sediment (Sites 12a-f, 12.1a-b, d-f, 13–15, 18–21, 23, 25a-f, 26, Table 2, Fig. 2i–j), on grey patches and bioturbated sediment (Sites 12.1c-e; 16–19, 22, 23, 25a-f, 26, Table 2, Fig. 2h–j), and in some cases spread adjacent to carbonate crusts. The area is also colonized by crabs, tube worms (Siboglinid), fishes, anemones and echinoids. Several articulated chemosymbiotic bivalve shells are present. Several clusters of dense bivalve beds are observed in this area, especially along the edges of the carbonate crusts. Patchily distributed, badly preserved bivalves encrusted by annelids are observed mostly along bacterial mats and altered carbonate crusts.

5. Discussion

5.1. The message from Lucinoma kazani

Salas and Woodside (2002) provided the first description of *Lucinoma kazani* on the Anaximander Mountains in the Eastern Mediterranean Basin at 1700–1709 m depth, in highly gas saturated mud-breccia deposits. We have recognized this species as the main component of bivalve beds, in the investigated areas of the PD (Figs. 1 and 2).

The *L. kazani* population in seepage sites of the PD consists of individuals characterized by different sizes (average 3–4 cm) and different degrees of preservation (Figs. 1–4). *Lucinoma kazani* (Fig. 4) is an infaunal thiotroph-associated lucinid (Duperron et al., 2007). It bears chemoautotrophic bacterial symbionts and lives in reducing sediments such as gas-saturated mud, with low-oxygen deep water. This species, is considered as evidence of living cold-seep communities in the Eastern Mediterranean (Salas and Woodside, 2002).

Although the growth rate of *L. kazani* is unknown, investigations on congeneric taxa (*L. aequizonata* (Suess, 1980) and *L. borealis* (Linnaeus, 1767), from suboxic water and sediments rich in hydrogen sulfide, revealed that *Lucinoma* spp. are motile bivalves able to dig from few mm down to about 20–50 cm into the sediment (Taylor and Glover, 2010) creating an extensive network of tunnels (Cary et al., 1989, and reference therein). They are able to use alternative, secondary sources of reduced carbon, other than from their symbionts, possibly from the pore-water, since their filtering and sorting efficiency is rather poor (Cary et al., 1989; Hentschel et al., 1993).

Depending on the consistent availability and sufficiency of the sulfide supply to the symbionts, the growth rate of the host bivalve can vary significantly. In *L. aequizonata* the growth rate in laboratory ranges from about 3 to about 12 µm day^{-1} (Cary et al., 1989). Under the hypothesis of a comparable growth rate for *L. kazani*, we could speculate that an individual about 3 cm long (the most common size observed in our samples) should not be younger than about 7 years.

The accumulation of dead, disarticulated shells on the seafloor is possibly the result of a mass mortality event due to a rapid change in the *Lucinoma* habitat, like a temporary interruption of the seepage, inducing the bivalves to move toward the water-sediment interface before their death. After death, presumably occurring at the sediment surface, the two valves of each individual may remain articulated for some months, and up to about one year, until the organic fibrous ligament decomposes (Cary et al., 1989; Gosling, 2015).

The tentative interpretation of the growth rate of *L. kazani* based on patterns observed in congeneric species does not allow for a precise age estimation, given the complex variables influencing bivalve growth. Nevertheless, the order of magnitude of several years required to reach the common size of about 3 cm of shell length is highly likely. Therefore, the occurrence of an autochthonous population of *L. kazani* with large individuals unequivocally testifies seepage continuity at least on a decadal time scale. The size and preservation of shells in an assemblage is not homogeneous (e.g., Callender and Powell, 1992; Basso and Corselli, 2007). In particular, the specimen 1a-b in Fig. 4 can be assigned to taphonomic grade 3 (well preserved, but disarticulated, with color fading to white, absence of dissolution). Accordingly, specimen 3a-b in Fig. 4 can be assigned to grade 1 (very bad preservation, broken, with greyish to brownish shell). A natural, autochthonous coastal mollusk population, in equilibrium with its environment, typically shows all degrees of shell size and preservation among dead mollusks (Basso and

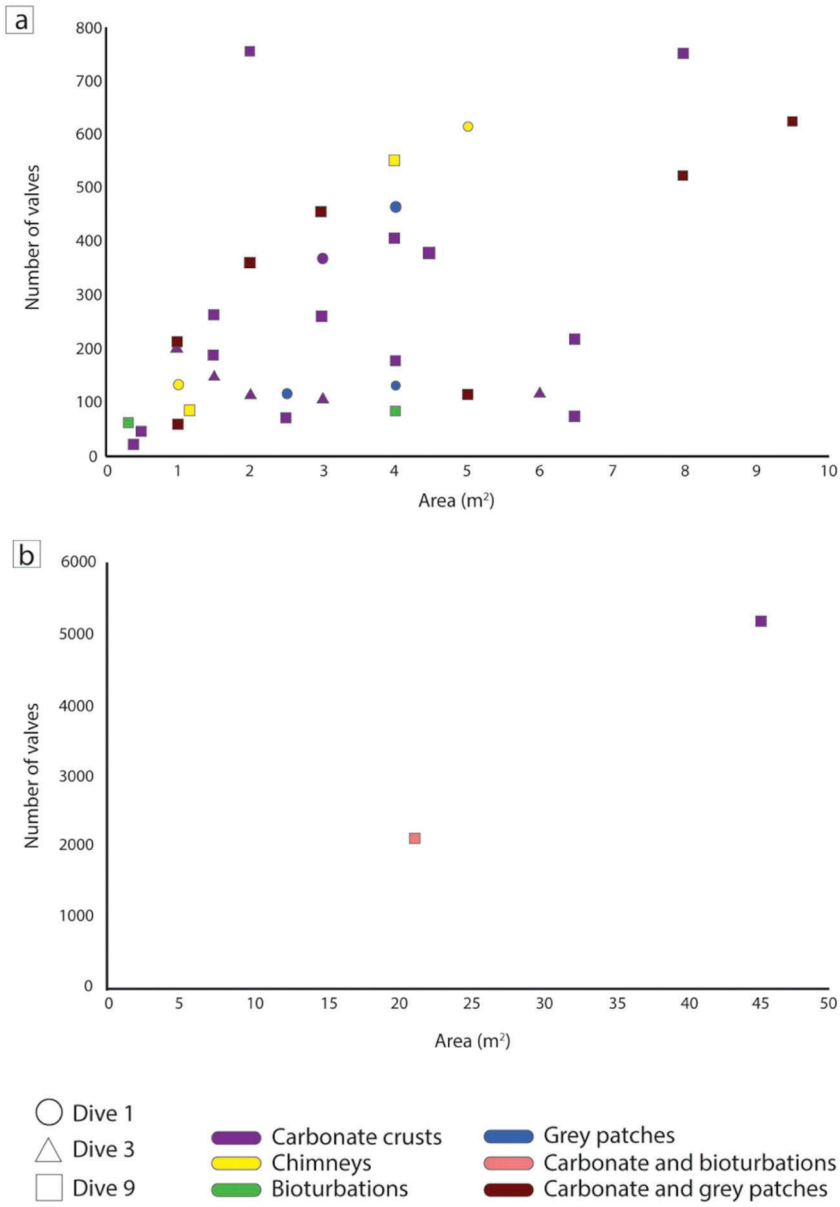

Fig. 5. Cross plots of valve numbers versus bivalve beds areas (Table 1). Colors refer to proximate seepage-related substrate, and symbols to the ROV dives. (a) Sites with maximum number 800 valves; (b) Sites with valve numbers exceeding 800. No clear relationship among dives, substrates and number of individuals is observed. (For interpretation of the references to color in this figure legend, the reader is referred to the Web version of this article.)

Corselli, 2007). However, in the peculiar and deep-sea seep environment that may be characterized by intermittent activity, the variable shell preservation due to different seep phases at different times cannot be ruled out. We cannot differentiate whether the accumulation of dead shells is due to one recent mass mortality event, or to the cumulative effect of multiple mortality events occurring over a longer time span. However, the not negligible sedimentation rate in the area (~20–35 cm/kyr in >900 m) would lead to the burial of shells after death. Moreover, different taphonomic grades may appear on coeval shells over a geologically very short time interval (Callender and Powell, 1992), and the taphonomic signature of the seep environment includes relatively fast color fading, shell corrosion and dissolution, and consequent fragmentation by mechanical weakening of shells (Callender and Powell, 1992).

The presence of articulated individuals suggests that they were still alive some months up to one year before they were observed with the ROV in 2016, which is the time span needed to decompose the ligament keeping the two valves together (Gosling, 2015). On the other hand, the observed mortality could be related to a change in the seepage quality and/or quantity, in turn controlled by a still unknown potential interplay of geological and environmental constraints.

5.2. *The role of chemosymbiotic bivalves in the PD*

At deep-sea cold seeps chemosynthetic primary production sustains very high biomass and biodiversity. Macrofaunal community structure and composition provide consistent indicators of fluid-flow behavior, deep-sea connectivity, evolutionary and biogeographic patterns (Van Dover et al., 2002; Portail et al., 2015). Particularly, bivalve beds are important hotspots of life compared to the surrounding environment. For these reasons, it is crucial to identify species distribution within this environment, the characteristic facies and to define the invertebrate assemblage associated with each habitat. Eastern Mediterranean seeps are characterized by low macro- and mega-faunal diversity with respect to other known seep communities in the world, possibly due to isolation of the basin after the Messinian Salinity Crisis (Danovaro et al., 2010).

In the PD region, bivalves are observed mainly associated with characteristic seepage substrate features including: authigenic carbonate crusts, chimney-like structures, bioturbations and grey patches (Fig. 2). As no gas bubbling was observed in the investigated area of the PD during the SEMSEEPS cruise, the presence of emissions and their intensities need to be estimated based on their geological and biological products (e.g., Aharon, 1994). The ROV observations revealed the presence of carbonate crusts, pavements and chimneys, which are relatively abundant within the surveyed areas. Many of the observed accumulations of shells occur along the margins of these crusts, and only a few shells are observed on top of the carbonates surfaces (Fig. 2a-f-g). Recent, but currently inactive, seepage sites may be indicated by the chimney-like structures filled with sediments and bivalve shells (Fig. 2c). However, the carbonates observed at the surface probably reflect several thousand years old occurrence of seepage, as it has been revealed by isotopic analysis of morphologically similar carbonates in the deep-sea fan of the Nile (Bayon et al., 2009). The observed carbonates themselves are therefore, probably not indicative of recent emissions. Thus, their observed association with presumably recent bivalves suggests continued focusing of the seepage through or in the vicinity of these carbonates.

Chemosymbiotic bivalves, gastropods, siboglinid tubeworms, bacterial mats, sea anemones, galatheid crabs and shrimps are described as typical benthic communities within fluid seeps, occurring in unconsolidated fine-grained sediments where authigenic carbonates are precipitated as crusts, pavements or concretions at the sediment/water interface (e.g., Gay et al., 2006, and reference therein). Accordingly, although no gas bubbling was observed, active seepage sites in the PD area can be inferred from the presence of intense bioturbation, grey patches, bacterial mats (Fig. 2d–j, Dive 1, Dive 3 and 9), siboglinid tubeworms and macrofaunal communities. As suggested by the comparative analysis conducted by Ritt et al. (2011) in the Nile Deep Sea Fan and by several other authors in other seep areas (e.g., Gay et al., 2006, and references therein), seepage activity supports benthic activity and biomass and biodiversity are 1-2 order of magnitude higher than in the surrounding oxygenated and oligotrophic deep-sea environments. Similar patterns are observed in the PD area, where a large difference between chemosymbiotic communities' hotspots and the surrounding environment occurs. Moreover, the variation in the distribution of seep fauna is generally related to spatial and/or temporal variations in the supply of sulfides, methane or other hydrocarbons (MacDonald et al., 1989; Wenger and Isaksen, 2002). Following Salas and Woodside (2002) the extension (Table 2; Figs. 2 and 3) of bivalve beds, the preservation state of the dead bivalves (Fig. 4) and the density of shells in different areas (Table 2; Fig. 3) testifies for a current or recent occurrence and activity of the PD area seeps.

As pointed out in several locations such as the Barbados prism (Olu et al., 1997) and the subduction zone of Japan (Ohta and Laubier, 1987), small clusters of dense bivalve beds (>150 ind/m^2) may be sustained by more intense and localized fluid flows (Sibuet and Olu-Le Roy, 2002, and reference therein), whereas dispersed clams may be sustained by widespread low flows. However, intermediate flux of methane and sulphide are considered by several authors to be the optimal condition that sustains the highest macrofaunal densities (Kiel, 2015; Guillon et al., 2017). There is growing evidence that macrofaunal community patterns are driven by both habitat heterogeneity and pattern of fluid flows even at the single pockmark scale, center versus margins (Zeppilli et al., 2012).

In the PD area, a causal link between the spatial distribution of bivalves and the activity of seepage is not straightforward. The bivalve beds areas are clustered or spread over wide areas (Table 1, Fig. 3). The largest surfaces characterized by dense clusters of dead bivalves were observed especially in Dive 9, close to carbonate crusts or above bacterial mats, where more active seepage seems to have been observed, while bivalves are less abundant around the carbonate crusts surveyed during Dive 3, where active seepage seemed less abundant.

These communities are important bioindicators of seepage, independently from the occurrence of visible gas bubbling, since the fauna is actually sensitive to the directly available dissolved seepage. Also, gas emissions may be intermittent or too weak to provide visual evidence (Ritt et al., 2011; Guillon et al., 2017). The problem concerning the absence of living specimens at cold seeps is not unique in the PD. The reason may be the insufficient sampling effort associated with the heterogeneous distribution of cold seep fauna, depending on the nutrient sources and the ecology of the different species. In addition, gas seeping at the seafloor is an intermittent phenomenon at different time scales controlling the continuous development of the chemosymbiotic fauna (e.g., Tryon and Brown, 2001; Raso et al., 2019).

6. Summary and conclusions

Despite the relatively small-investigated area, our observations enable the following conclusions: bivalve beds in the Palmahim Disturbance (PD) area, offshore Israel, are dominated by the chemosymbiotic infaunal bivalve *Lucinoma kazani*. A total area of 208.4 m^2 of bivalve beds was identified, with densities ranging from 11 to 377 valves m^{-2}, in a total recorded transect length of 50 km.

The link between areal distribution of the bivalve beds and seep activity is not straightforward in the PD. However, the highest density of bivalves observed in the largest area seems to be related to active seepage. In presence of bacterial mats the seeps may still be active, although no bubbling was observed.

The distribution of bivalve beds is not homogeneous and the amount of dead shells is very different from site to site. Where valves are abundant, also articulated individuals are present (e.g., Dive 9, Fig. 2), indicating that these individuals were alive up to one year before the ROV observations due to the post-mortem preservation time of the bivalve ligament (months to one year). This implies also that the seepage necessary to support their life was active in very recent times.

The accumulation of dead and disarticulated shells may result from mass mortality episode due to changes in the *Lucinoma* habitat. In particular, temporary interruption or reduction in seepage activity may have induced the bivalves to move toward the water-sediment interface before their death. Further quantitative studies on their preservation state will clarify if specimens with different preservation state are linked to different phases of the intermittent seepage activity at different times.

Based on the estimated growth rate of *Lucinoma kazani*, the seepage should have lasted for at least one decade, before the reduction/cessation that induced the observed *L. kazani* mortality event. Our study confirms that chemosymbiotic bivalve beds can be used as proxy for understanding the past distribution pattern of the emissions at the seafloor in the PD. However, more investigations are needed to describe the pattern of geographic and subsurface distribution, to quantify the amount of gas seepages in the region, to finally provide a baseline for a quantification of emission rates vs the distribution, abundance and individual size of these bivalves.

Authors contribution

VB performed the analysis on the bivalve distribution, wrote the paper.

DB conceived and designed the analysis, wrote the paper.

SS contributed to the interpretation, wrote the paper and obtained funding from the Swiss National Science Foundation for shore-based studies that made this research possible.

AR cruise project proponent and SEMSEEP cruise co-chief scientist, contributed analysis tools.

AN contributed to the maps production.

YM cruise project proponent and SEMSEEP cruise co-chief scientist, contributed to the maps production and spatial analysis, wrote the paper.

Acknowledgement

We warmly thank the scientific and technical crew of the R/V AEGAEO who helped during sampling operations. The EUROFLEETS2 SEMSEEP cruise was funded by the European Union FP7 Programme under grant agreement n° 312762. The Swiss National Science Foundation grant Ref. 200021_175587 provided funding for shorebased investigations that made this research possible. The Fonds de recherche n° 609 of the University of Fribourg, the Helmsley Charitable Trust and Charney School of Marine Sciences, University of Haifa, Israel Oceanographic and Limnological Research provided additional support for the cruise. Thanks to the Israeli Ministry of Infrastructure, Energy and Water for IOLR support, Yoni Esakow and Coral Group Ltd. for donating their in-port support, Paradigm for geophysical software sponsorship, the State of Israel Ministry of Foreign Affairs, through their Embassy in Cyprus and the Embassy of Switzerland in Cyprus, for their dedicated backing. DB acknowledges Project MIUR – Dipartimenti di Eccellenza 2018–2022.

Appendix A. Supplementary data

Supplementary data to this article can be found online at https://doi.org/10.1016/j.dsr2.2019.104664.

References

Aharon, P., 1994. Geology and biology of modern and ancient submarine hydrocarbon seeps and vents: an introduction. Geo Mar. Lett. 14 (2), 69–73.
Almogi-Labin, A., Bar-Matthews, M., Shriki, D., Kolosovsky, E., Paterne, M., Schilman, B., Ayalon, A., Aizenshtat, Z., Matthews, A., 2009. Climatic variability during the last~ 90 ka of the southern and northern Levantine Basin as evident from marine records and speleothems. Quat. Sci. Rev. 28 (25-26), 2882–2896.
Aloisi, G., Bouloubassi, I., Heijs, S.K., Pancost, R.D., Pierre, C., Damsté, J.S.S., Gottschal, J.C., Forney, L.J., Rouchy, J.-M., 2002. CH4-consuming microorganisms and the formation of carbonate crusts at cold seeps. Earth Planet. Sci. Lett. 203 (1), 195–203.
Barnes, R.O., Goldberg, E.D., 1976. Methane production and consumption in anoxic marine sediments. Geology 4 (5), 297–300.
Basso, D., Corselli, C., 2007. Molluscan paleoecology in the reconstruction of coastal changes. In: The Black Sea Flood Question: Changes in Coastline, Climate, and Human Settlement. Springer, pp. 23–46.
Basso, D., Thomson, J., Corselli, C., 2004. Indications of low macrobenthic activity in the deep sediments of the eastern Mediterranean Sea. Sci. Mar. 68 (S3), 53–62.
Bayon, G., Henderson, G.M., Bohn, M., 2009. U–Th stratigraphy of a cold seep carbonate crust. Chem. Geol. 260 (1-2), 47–56.
Blumenberg, M., Walliser, E.O., Taviani, M., Seifert, R., Reitner, J., 2015. Authigenic carbonate formation and its impact on the biomarker inventory at hydrocarbon seeps–A case study from the Holocene Black Sea and the Plio-Pleistocene Northern Apennines (Italy). Mar. Pet. Geol. 66, 532–541.
Boetius, A., Ravenschlag, K., Schubert, C.J., Rickert, D., Widdel, F., Gieseke, A., Amann, R., Jorgensen, B.B., Witte, U., Pfannkuche, O., 2000. A marine microbial consortium apparently mediating anaerobic oxidation of methane. Nature 407 (6804), 623.
Boetius, A., Wenzhöfer, F., 2013. Seafloor oxygen consumption fuelled by methane from cold seeps. Nat. Geosci. 6 (9), 725.
Callender, W.R., Powell, E.N., 1992. Taphonomic signature of petroleum seep assemblages on the Louisiana upper continental slope: recognition of autochthonous shell beds in the fossil record. Palaios 388–408.
Cary, S., Vetter, R., Felbeck, H., 1989. Habitat characterization and nutritional strategies of the endosymbiont-bearing bivalve *Lucinoma*. Mar. Ecol. Prog. Ser. 55, 31–45.
Coleman, D.F., Austin Jr., J.A., Ben-Avraham, Z., Makovsky, Y., Tchernov, D., 2012. Seafloor pockmarks, deepwater corals, and cold seeps along the continental margin of Israel. Oceanography 25, 40–41.
Cordes, E.E., Cunha, M.R., Galeron, J., Mora, C., Olu-Le Roy, K., Sibuet, M., Van Gaever, S., Vanreusel, A., Levin, L.A., 2010. The influence of geological, geochemical, and biogenic habitat heterogeneity on seep biodiversity. Mar. Ecol. 31, 51–65.
Corselli, C., Basso, D., 1996. First evidence of benthic communities based on chemosynthesis on the Napoli mud volcano (Eastern Mediterranean). Mar. Geol. 132, 227–239.
Danovaro, R., Corinaldesi, C., D'Onghia, G., Galil, B., Gambi, C., Gooday, A.J., Lampadariou, N., Luna, G.M., Morigi, C., Olu, K., Polymenakou, P., Ramirez-Llodra, E., Sabbatini, A., Sardà, F., Sibuet, M., Tselepides, A., 2010. Deep-sea biodiversity in the Mediterranean Sea: the known, the unknown, and the unknowable. PLoS One 5 (8), e11832.
Davies, D.J., Staff, G.M., Callender, W.R., Powell, E.N., 1990. Description of a Quantitative Approach to Taphonomy and Taphofacies Analysis: All Dead Things Are Not Created Equal, vol. 5. The Paleontological Society Special Publications, pp. 328–350.
Duperron, S., Fiala-Medioni, A., Caprais, J.-C., Olu, K., Sibuet, M., 2007. Evidence for chemoautotrophic symbiosis in a Mediterranean cold seep clam (Bivalvia: Lucinidae): comparative sequence analysis of bacterial 16S rRNA, APS reductase and RubisCO genes. FEMS Microbiol. Ecol. 59 (1), 64–70.
Foucher, J.P., Westbrook, G.K., Boetius, A., Ceramicola, S., Dupré, S., Mascle, J., Mienert, J., Pfannkuche, O., Pierre, C., Praeg, D., 2009. Structure and drivers of cold seep ecosystems. Oceanography 22 (1), 92–109.
Garfunkel, Z., Almagor, G., Arad, A., 1979. The Palmahim disturbance and its regional setting. Geol. Surv. Isr. Bull. 72.
Gay, A., Lopez, M., Ondreas, H., Charlou, J.-L., Sermondadaz, G., Cochonat, P., 2006. Seafloor facies related to upward methane flux within a Giant Pockmark of the Lower Congo Basin. Mar. Geol. 226 (1-2), 81–95.
Gontharet, S., Pierre, C., Blanc-Valleron, M.M., Rouchy, J.M., Fouquet, Y., Bayon, G., Foucher, J.P., Woodside, J., Mascle, J., Party, T.N.S., 2007. Nature and origin of diagenetic carbonate crusts and concretions from mud volcanoes and pockmarks of the Nile deep-sea fan (eastern Mediterranean Sea). Deep Sea Res. Part II Top. Stud. Oceanogr. 54 (11-13), 1292–1311.
Gosling, E., 2015. Marine Bivalve Molluscs, second ed. John Wiley and Sons, UK.
Guillon, E., Menot, L., Decker, C., Krylova, E., Olu, K., 2017. The vesicomyid bivalve habitat at cold seeps supports heterogeneous and dynamic macrofaunal assemblages. Deep Sea Res. Oceanogr. Res. Pap. 120, 1–13.
Gvirtzman, Z., Reshef, M., Buch-Leviatan, O., Groves-Gidney, G., Karcz, Z., Makovsky, Y., Ben-Avraham, Z., 2015. Bathymetry of the Levant basin: interaction of salt-tectonics and surficial mass movements. Mar. Geol. 360, 25–39.
Hentschel, U., Cary, S.C., Felbeck, H., 1993. Nitrate respiration in chemoautotrophic symbionts of the bivalve *Lucinoma aequizonata*. Mar. Ecol. Prog. Ser. 94, 35–41.
Hsü, K.J., Montadert, L., Bernoulli, D., Cita, M.B., Erickson, A., Garrison, R.E., Kidd, R.B., Mèlierés, F., Muller, C., Wright, R., 1977. History of the Mediterranean salinity crisis. Nature 267 (5610), 399.
Huguen, C., Foucher, J.P., Mascle, J., Ondréas, H., Thouement, M., Gontharet, S., Stadnitskaia, A., Pierre, C., Bayon, G., Loncke, L., Bouloubassi, I., de Lange, G., Caprais, J.C., Fouquet, Y., Woodside, J., Dupré, S., Boetius, A., NAUTINIL Scientific Party, 2009. Menes caldera, a highly active site of brine seepage in the Eastern Mediterranean sea: "In situ" observations from the NAUTINIL expedition 2003. Mar. Geol. 261 (1-4), 138–152.
Kiel, S., 2015. Did shifting seawater sulfate concentrations drive the evolution of deep-sea methane-seep ecosystems? Proc. R. Soc. Biol. Sci. 282 (1804), 20142908.
Kiel, S., 2016. A biogeographic network reveals evolutionary links between deep-sea hydrothermal vent and methane seep faunas. Proc. R. Soc. Biol. Sci. 283 (1844), 20162337.
Levin, L.A., 2005. Ecology of cold seep sediments: interactions of fauna with flow, chemistry and microbes. In: Oceanography and Marine Biology. CRC Press, pp. 11–56.
Levin, L.A., Baco, A.R., Bowden, D.A., Colaco, A., Cordes, E.E., Cunha, M.R., Demopoulos, A.W.J., Gobin, J., Grupe, B.M., Le, J., Metaxas, A., Netburn, A.N., Rouse, G.W., Thurber, A.R., Tunnicliffe, V., Lee Van Dover, C., Vanreusel, A., Watling, L., 2016. Hydrothermal vents and methane seeps: rethinking the sphere of influence. Front. Mar. Sci. 3, 72.
Loncke, L., Gaullier, V., Mascle, J., Vendeville, B., Camera, L., 2006. The Nile deep-sea fan: an example of interacting sedimentation, salt tectonics, and inherited subsalt paleotopographic features. Mar. Pet. Geol. 23 (3), 297–315.
Lonsdale, P., 1977. Clustering of suspension-feeding macrobenthos near abyssal hydrothermal vents at oceanic spreading centers. Deep-Sea Res. 24 (9), 857–863.
MacDonald, I.R., Boland, G.S., Baker, J.S., Brooks, J.M., Kennicutt, M.C., Bidigare, R.R., 1989. Gulf of Mexico hydrocarbon seep communities. Mar. Biol. 101 (2), 235–247.
Makovsky, Y., Rüggeberg, A., Bialik, O., Foubert, A., Almogi-Labin, A., Alter, Y., Bampas, V., Basso, D., Feenstra, E., Fentimen, R., Friedheim, O., Hall, E., Hazan, O., Herut, B., Kallergis, E., Karageorgis, A., Kolountzakis, A., Manousakis, L., Nikolaidis, M., Pantazoglou, F., Rahav, E., Renieris, P., Schleinkofer, N., Sisma Ventura, G., Stasnios, V., Weissman, A., the EuroFLEETS2 SEMSEEP Participants, 2017. South East Mediterranean SEEP Carbonate. R/V Aegaeo Cruise EuroFLEETS2 SEMSEEP, pp. 1–38.
Ohta, S., Laubier, L., 1987. Deep biological communities in the subduction zone of Japan from bottom photographs taken during "Nautile" dives in the Kaiko project. Earth Planet. Sci. Lett. 83 (1-4), 329–342.
Olu, K., Lance, S., Sibuet, M., Henry, P., Fiala-Médioni, A., Dinet, A., 1997. Cold seep communities as indicators of fluid expulsion patterns through mud volcanoes seaward of the Barbados accretionary prism. Deep Sea Res. Oceanogr. Res. Pap. 44 (5), 811–841.
Olu-Le Roy, K., Sibuet, M., Fiala-Médioni, A., Gofas, S., Salas, C., Mariotti, A., Foucher, J. P., Woodside, J., 2004. Cold seep communities in the deep eastern Mediterranean Sea: composition, symbiosis and spatial distribution on mud volcanoes. Deep Sea Res. Oceanogr. Res. Pap. 51 (12), 1915–1936.
Olu-Le Roy, K., Caprais, J., Fifis, A., Fabri, M., Galeron, J., Budzinsky, H., Le Ménach, K., Khripounoff, A., Ondréas, H., Sibuet, M., 2007. Cold-seep assemblages on a giant pockmark off West Africa: spatial patterns and environmental control. Mar. Ecol. 28 (1), 115–130.
Paull, C.K., Hecker, B., Commeau, R., Freeman-Lynde, R., Neumann, C., Corso, W., Golubic, S., Hook, J., Sikes, E., Curray, J., 1984. Biological communities at the Florida Escarpment resemble hydrothermal vent taxa. Science 226 (4677), 965–967.
Portail, M., Olu, K., Escobar-Briones, E., Caprais, J.-C., Menot, L., Waeles, M., Cruaud, P., Sarradin, P.-M., Godfroy, A., Sarrazin, J., 2015. Comparative study of vent and seep macrofaunal communities in the Guaymas Basin. Biogeosciences 12 (18), 5455–5479.

Raso, J.E.G., García-Muñoz, J.E., Mateo-Ramírez, A., González, N.L., Fernández-Salas, L. M., Rueda, J.L., 2019. Decapod crustaceans Eucalliacidae in chemoautotrophic bathyal bottoms of the Gulf of Cadiz (Atlantic Ocean), environmental characteristics and associated communities. J. Mar. Biol. Assoc. U. K. 99 (2), 437–444.
Ritger, S., Carson, B., Suess, E., 1987. Methane-derived authigenic carbonates formed by subduction-induced pore-water expulsion along the Oregon/Washington margin. Geol. Soc. Am. Bull. 98 (2), 147–156.
Ritt, B., Sarrazin, J., Caprais, J.C., Noël, P., Gauthier, O., Pierre, C., Henry, P., Desbruyeres, D., 2010. First insights into the structure and environmental setting of cold-seep communities in the Marmara Sea. Deep Sea Res. Oceanogr. Res. Pap. 57 (9), 1120–1136.
Ritt, B., Pierre, C., Gauthier, O., Wenzhöfer, F., Boetius, A., Sarrazin, J., 2011. Diversity and distribution of cold-seep fauna associated with different geological and environmental settings at mud volcanoes and pockmarks of the Nile Deep-Sea Fan. Mar. Biol. 158 (6), 1187–1210.
Rubin-Blum, M., Antler, G., Turchyn, A.V., Tsadok, R., Goodman-Tchernov, B.N., Shemesh, E., Austin, J.A., Coleman, D.F., Makovsky, Y., Sivan, O., Tchernov, D., 2014. Hydrocarbon-related microbial processes in the deep sediments of the eastern mediterranean Levantine Basin. FEMS Microbiol. Ecol. 87 (3), 780–796.
Sahling, H., Rickert, D., Lee, R.W., Linke, P., Suess, E., 2002. Macrofaunal community structure and sulfide flux at gas hydrate deposits from the Cascadia convergent margin, NE Pacific. Mar. Ecol. Prog. Ser. 231, 121–138.
Salas, C., Woodside, J., 2002. *Lucinoma kazani* n. sp. (Mollusca: Bivalvia): evidence of a living benthic community associated with a cold seep in the Eastern Mediterranean Sea. Deep Sea Res. Oceanogr. Res. Pap. 49 (6), 991–1005.
Scarponi, D., Kowalewski, M., 2004. Stratigraphic paleoecology: bathymetric signatures and sequence overprint of mollusk associations from upper Quaternary sequences of the Po Plain. Italy. *Geology* 32 (11), 989–992.
Schlitzer, R., 2018. Ocean data view. https://odv.awi.de.
Sibuet, M., Olu-Le Roy, K., 2002. Cold seep communities on continental margins: structure and quantitative distribution relative to geological and fluid venting patterns. In: Ocean Margin Systems. Springer, Berlin, Heidelberg, pp. 235–251.
Suess, E., 1980. Particulate organic carbon flux in the oceans—surface productivity and oxygen utilization. Nature 288 (5788), 260–263.
Taviani, M., Angeletti, L., Ceregato, A., Foglini, F., Froglia, C., Trincardi, F., 2013. The Gela Basin pockmark field in the strait of Sicily (Mediterranean Sea): chemosymbiotic faunal and carbonate signatures of postglacial to modern cold seepage. Biogeosci. Discuss. 10 (10), 967–1009. https://doi.org/10.5194/bdg-10-967-2013.
Taviani, M., 2014. Marine chemosynthesis in the Mediterranean Sea. In: The Mediterranean Sea. Springer, Dordrecht, pp. 69–83.
Taylor, J.D., Glover, E.A., 2010. Chemosymbiotic bivalves. In: The Vent and Seep Biota. Springer, Dordrecht, pp. 107–135.
Tryon, M.D., Brown, K.M., 2001. Complex flow patterns through Hydrate Ridge and their impact on seep biota. Geophys. Res. Lett. 28 (14), 2863–2866.
Van Dover, C.L., German, C., Speer, K.G., Parson, L., Vrijenhoek, R., 2002. Evolution and biogeography of deep-sea vent and seep invertebrates. Science 295 (5558), 1253–1257.
Van Dover, C.L., Aharon, P., Bernhard, J.M., Caylor, E., Doerries, M., Flickinger, W., Gilhooly, W., Goffredi, S.K., Knick, K.E., Macko, S.A., Rapoport, S., Raulfs, E.C., Ruppel, C., Salerno, J.L., Seitz, R.D., Sen Gupta, B.K., Shank, T., Turnispeed, M., Vrijenhoek, R., 2003. Blake Ridge methane seeps: characterization of a soft-sediment, chemosynthetically based ecosystem. Deep Sea Res. Part I 50 (2), 281–300.
Vanreusel, A., Andersen, A.C., Boetius, A., Connelly, D., Cunha, M.R., Decker, C., Hilario, A., Kormas, A.K., Maignien, L., Olu, K., Ritt, B., Rodrigues, C., Sarrazin, J., Tyler, P., van Gaever, S., Vanneste, H., Pachiadaki, M., 2009. Biodiversity of cold seep ecosystems along the European margins. Oceanography 22 (1), 110–127.
Wenger, L.M., Isaksen, G.H., 2002. Control of hydrocarbon seepage intensity on level of biodegradation in sea bottom sediments. Org. Geochem. 33 (12), 1277–1292.
Werne, J.P., Haese, R.R., Zitter, T., Aloisi, G., Bouloubassi, I., Heijs, S., Fiala-Medioni, A., Pancost, R., Sinnighe Damste, J.S., de Lange, G., Gottschal, J.C., Foucher, J.P., Mascle, J., Woodside, J., Forney, L.J., MEDINAUT, MEDINETH Scientific Parties, 2004. Life at cold seeps: a synthesis of biogeochemical and ecological data from Kazan mud volcano, eastern Mediterranean Sea. Chem. Geol. 205 (3-4), 367–390.
Woodside, J., Ivanov, M., Limonov, A., 1998. Shallow gas and gas hydrates in the Anaximander Mountains region, eastern Mediterranean Sea. Geol. Soc. Lond. Spec. Publ. 137 (1), 177–193.
Zeppilli, D., Canals, M., Danovaro, R., 2012. Pockmarks enhance deep-sea benthic biodiversity: a case study in the western Mediterranean Sea. Divers. Distrib. 18 (8), 832–846.
Zitter, T.A.C., Huguen, C., Woodside, J.M., 2005. Geology of mud volcanoes in the eastern Mediterranean from combined sidescan sonar and submersible surveys. Deep Sea Res. Oceanogr. Res. Pap. 52 (3), 457–475.